EXPERIMENTAL STUDY OF METAL CUSHION PADS FOR HIGH SPEED RAILWAYS.

Isidro A. CARRASCAL[1], Alejandro PÉREZ[2], José A. CASADO[1], Soraya DIEGO[1], Juan A. POLANCO[1], Diego FERREÑO[1], Juan J. MARTÍN[2].

[1] LADICIM (Laboratory of Science and Engineering of Materials), University of Cantabria. E.T.S. de Ingenieros de Caminos, Canales y Puertos, Av. Los Castros 44, 39005 Santander, Spain.

[2]TEJASA TC S.L. C/ La Industria, 77. Parque Industrial Tirso Gonzalez, N 21 y 22-6, 39610 El Astillero (Cantabria), Spain.

ABSTRACT

The widespread use of railway concrete sleepers / slab track has led to the evolution of fastening systems towards the use of elastic rail pads. Pads are interposed between the rail and the sleeper as damping elements to minimize the transmission of shocks and vibrations to the sleeper, this function being of particular importance for high-speed railways. Polymeric materials have been extensively used to manufacture resilient rail pads. Plastics, however, suffer from a series of intrinsic limitations since the environmental agents (UV rays, temperature, air humidity, etc.) as well as the compressive fatigue loads they are subjected to, negatively affect their mechanical properties over time. This study proposes the use of a novel solution, the so-called 'metal cushion' pads, as a reliable alternative to polymer pads. Metal cushion pads are made of stainless steel wire, knitted, embossed and cold-pressed down into a mold to achieve the required shape and size. The thorough experimental scope carried out in this research includes the following tests: (i) static and dynamic stiffness, (ii) fatigue aging, (iii) electrical resistance and, (iv) corrosion resistance. The values of static and dynamic stiffness are very similar to those obtained with other traditional polymers such as EVA and TPE-M. In addition, it has been found that the stiffness of the metallic solution can be modified by changing the diameter and density of the wire. In the case of fatigue aging, the foremost wearing suffered by the metal cushion pads occurs mainly in the early cycling stages, although the total damage is comparable to that of the traditional solutions. The electrical resistance of the metal cushion does not fulfill the requirements demanded by the international standards; however, its behavior is satisfactory if the metallic solution is combined with a thin plastic sheet. Finally, the metal samples have passed the corrosion test in a saline environment without showing any signs of corrosion damage.

Keywords: *rail pads; metal cushion; stainless steel; stiffness; fatigue; electrical resistance; corrosion resistance.*

1. INTRODUCTION.

The development and implementation of the high performance railway has been accompanied by a complete revolution in the design and manufacture of the elements of the railway superstructure. Currently, high-speed railways are based on the use of concrete sleepers (or, in some cases, slab track) and complex fastening systems between the concrete and the rails. Aiming at relieving the excessive stiffness of concrete (which can be up to five times higher than those made of wood [1]),elastic pads are placed between them and the rails. Rail pads play an indispensable role within the fastening systems since they cushion the shocks and vibrations caused by the transit of the train wheels. As a new track is subjected to repetitive loads caused by the transit of train wheels, it undergoes plastic deformations that grow over time until the system reaches the steady state. Then, a true stable elastic regime is established and the system behaves like a homogeneous solid [2], [3]. Formula (1), proposed in [3], allows the influence of the stiffness of the rail pads, k_p, and the ballast platform, k_{bp}, on the overall stiffness of the rail's support, k_s, to be determined:

$$k_s = \frac{k_p.k_{bp}}{k_p+k_{bp}} \qquad (1)$$

A high value of the stiffness of the rail pads will increase the dynamic overloads due to unsprung masses, accelerating the deterioration of the track; in contrast, low stiffness will cause the sinking of the track, leading to a noticeable increase in the stress state of the rails [4] [5]. Consequently, it is essential to define the range of stiffness values that lead to the adequate performance of the fastening system [6] [7].

Without claiming to be exhaustive, a review of the literature on the influence of the stiffness of the pad on the performance of the track is summarized next.

- The stiffness of the rail pads has been related to the deterioration of the ballast. Thus, countries such as Germany, Spain, France or Greece initially adopted high-stiff rail pads for high-speed lines (k_p = 400 - 500 kN / mm) which, combined with the intrinsic stiffness of the rail substructure (several layers of gravel in the base), brought about the deterioration of the ballast. Because of this, a lower stiffness of the rail pads (60 - 100 kN / mm) was chosen to reduce the total rigidity of the assembly [1] [4].
- According to [8], the variation in the overall stiffness between rail sections may lead to a 40% increase in the rail stress, due to the differential vertical displacements that take place.
- The reduction of the stiffness of the plates results in a decrease in the stress state of the sleepers. High pad high stiffness provoked cases of fractured sleepers, as described in [9]. Reducing the pad's stiffness from 250 to 40 kN/mm leads to a 20% decrease in the maximum stress of the sleeper.
- Theoretical studies on vibration and noise (based on different mechanical models such as Maxwell [10], Kelvin [11] or Poynting–Thomson [12]) have been carried out to study the material performance [13] [14]. As a rule of thumb, the higher the pad's stiffness the higher the transmission of noise due to the transit of trains. On the contrary, large damping reduces the transmission of vibrations into the sleeper [15]. The influence of stiffness on the amount of transmitted sound level has been analyzed in [16]. According to this study, low stiffness allows the transmission of sound frequencies below 250 Hz, below 450 Hz for medium stiffness and 800 Hz for high stiffness.
- The non-linear mechanical response of the rail pads may have detrimental effects regarding their ability to isolate vibrations. It was shown that the second and third modes of vibration could be included in the

frequency range (300 – 600 Hz) which is associated with rail corrugation effects; moreover, under some conditions, dangerous resonances may appear when rolling stocks pass over [10].

- Previous studies [17] have compared the rail pad's ability for energy absorption with its stiffness. HDPE plates can absorb up to 50%of the total incoming shock energy. The same conclusions are present in [18], in this case for TPE plates, 7.00 mm thick, with a stiffness of 100 kN/mm.
- The short-term dynamic effects on the rail, caused by the stiffness of the pads, are accompanied by some forms of long-term damage, such as the so-called rail corrugation. This term refers to the quasi-sinusoidal irregularities of the wheels and rails, caused by the mechanical interactions (vibrations and dynamic loadings) between them. Rail corrugation is also related with rail pad stiffness, so that the higher the stiffness, the higher the presence of this pernicious effect [19]. The experimental data collected in [20] show that a reduction in rail pad stiffness from 90 to 60 kN/mm, leads to a 55% decrease in corrugation amplitude and length.

Several polymeric materials such as EPDM, TPE, TPU and rubber have been extensively used to manufacture rail pads [21] [22], in particular for high speed railway tracks. Unfortunately, several environmental agents, UV rays and temperature being the most common, may degrade the stiffness of these pads. Previous studies were focused on improving the aging performance of these materials. For instance, in [23] tiuram and sulfide curing treatments on SBR rail pads were compared, concluding that the latter provides the best performance. Setting aside environmental issues, as a matter of fact, the durability of the rail pads is always limited because of the repetitive loads and impacts coming from the passage of rolling stocks. Several studies confirm this statement; for instance, in [24] the loading effect in a 5.5 mm thick HDPE rail pad was measured, observing a stiffness deterioration of 13 kN/mm and a damping degradation of 41 N·s/m. Moreover, in [25] a 44% stiffness aging increment was observed in a TPE rail pad after 3 years under in-service conditions. Fatigue is another cause of material deterioration leading to the increase in stiffness [26] [27] [28]. This phenomenon is accompanied by a reduction in the ability of the part to dissipate the energy coming from load-unload cycles. The experimental data show that a fatigue increase of stiffness of 18% reduces the ability for energy absorption by 40% [27]. In addition, the fatigue loading also produced a thickness reduction of the rail pad [29].

In conclusion, the polymeric materials currently used as rail pads may suffer from severe limitations in the long run because of the modifications that their stiffness undergo as a result of the environmental conditions and the loads they are subjected to. For these reasons, the pads must be replaced over time, which negatively affects the economic performance of the track, as well as the quality of the service. These are the circumstances that motivate the present study, which is aimed at developing and validating, relying on the experimental results, a novel solution capable of overcoming the intrinsic limitations of polymeric materials. Metallic rail pads have been employed in the past, particularly in the form of plates between the rails and the wooden sleepers. This option is not applicable for concrete sleepers, due to the excessive stiffness of this solution. In this sense, we propose the use of the so-called *metallic cushion pads* (also called *metal-rubber damper*), made of stainless steel, as a superior alternative both from the mechanical point of view and from the perspective of the durability of the material against loads or environmental conditions. As proved in this study, the metal cushion-based solution allows the designer to select the most suitable stiffness to guarantee the adequate performance of the system. Metal cushion is advantageous as

compared to polymers since it provides a uniform and environmentally independent performance, as well as an improved dynamic behavior regarding noise and vibrations.

The experimental campaign in this study consisted in comparing the response of six polymeric solutions, currently employed in actual railway tracks, against the behavior of themetal cushion pads. The experimental scope developed is briefly summarized hereafter. The static and dynamic stiffness of the different solutions was obtained following the guidelines of the international standards EN 13146-9+A1 [30] y EN 13481-2 [31], respectively. In order to assess the mechanical aging derived from the application of repetitive loads, static and dynamic stiffness were determined again after subjecting the pads, respectively to $3.5 \cdot 10^5$ and $3 \cdot 10^6$ fatigue cycles, following the standard EN 13146-4+A1 [32]. Likewise, a series of complementary aging tests was carried out after modifying the density and the thickness of the filament of the metallic rubber, in order to evaluate their influence on the stiffness of the pad. The intrinsic electrical conductivity of metals and their susceptibility to corrosion represent, a priori, two foreseeable limitations for the implementation of metal cushion pads. For this reason, a series of tests were performed to obtain the electrical resistance, following the standard EN 13146-5 [33], as well as accelerated corrosion tests in the salt spray chamber, in agreement with the standards EN 13146-4 [32] and EN ISO 9227 [34].

As indicated, the scope of this work focuses on the mechanical competence and electrical insulation ability of the proposed solution. Other relevant aspects, such as its performance to attenuate impacts and/or vibrations have not been analyzed and their study is postponed for future research.

2.- MATERIALS AND METHODS.

2.1.- Material.

The six polymeric materials involved in this study are described hereafter; four of them are currently present in numerous railway lines whereas the remaining two are prototypes:

- TPE-M: Polyester elastomer thermopolymer (Hytrel™), medium stiffness. Used on PAE-2 rail pads [35], with a thickness of 7 mm, with oblong shaped protrusions and a hardness of 47 HS-D. Solution currently adopted in the Spanish high speed railways.
- TPE-S: polyester elastomer (Hytrel™) thermopolymer, reduced stiffness. Used in a 9 mm thick pad with oblong shaped protrusions and a hardness of 45 HS-D. Prototype.
- EPDM: ethylene-propylene copolymer, 7 mm thick, solid plate without protrusions, with a hardness of 21 HS-D. Solution adopted in Saudi Arabia high speed railways.
- TPU: Polyurethane elastomer thermopolymer, 9 mm thick. Solid pad without protrusions and a hardness of 30 HS-D. Solution adopted in Mexican railroads.
- NFU: Out-of-use tire, with grain size less than 2 mm, bonded with resin to form a 7.5 mm thick pad. Prototype.
- EVA: Ethylene-vinyl acetate. 6mm thick solid pad without protrusions and a hardness of 46 HSD. Solution adopted in the first Spanish high-speed line between Madrid and Sevilla.

Samples made of these materials with a size of 45 x 42 mm^2 were cut from larger plates. Figure 1 shows a photograph that includes one sample of each type.

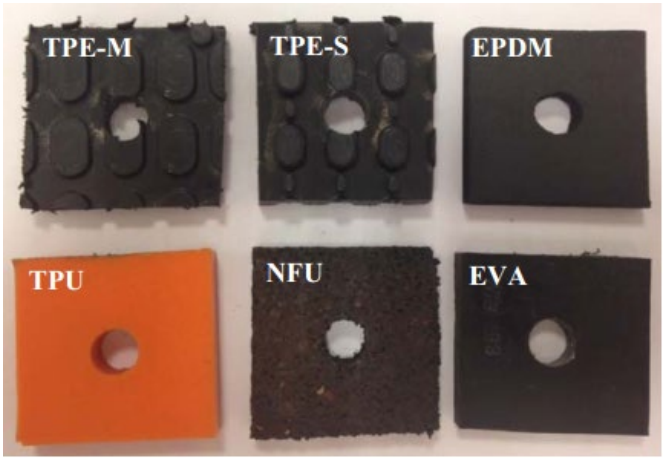

Figure1. Rail pad standard solutions, fabricated with different materials, used in the study to compare with the metal cushion damper alternative.

Figure 2 shows one of the metal cushion samples involved in this study. It has been provided and produced by Silentflex™. This solution is made of stainless steel wire, knitted, embossed and cold-pressed down into a mold to achieve the required shape and size. A first advantage of this solution comes from the fact that its geometry is very versatile since the pads are manufactured by molding. Metal cushion pads are 100% stainless steel (AISI-302, AISI-304 or AISI-316 for highly corrosive environments). They are not affected by hydrocarbons, water, or UV rays, among others, and their elastic behavior is guaranteed in a wide range of temperatures (between -50ºC and 300ºC). In fact, specific metal cushion dampers can be fabricated for industrial applications with temperatures ranging between -70°C and +400°C. This type of solutions has proved its suitability for acoustic and vibration insulation; for instance, they have been used to isolate rotary machines whose angular speed is higher than 2000 rpm [36]. The dimensions of the metal cushion damper shown in Figure 2 are (length x width x height) of 45x42x7 mm^3, with a central Φ10 mm hole. Note that the surface dimensions are the same as those of the polymer plates shown in Figure 1. Metal cushion materials presumably entail a disadvantage since they provide a noticeably lower electrical resistance than polymers. This obviously affects the results of the electrical resistance tests (EN 13146-5 [33]); this subject is covered in section 4.3.

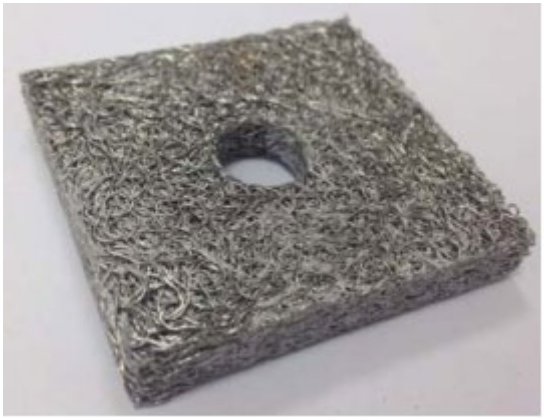

Figure 2. Sample of a metal cushion pad.

Aiming at obtaining different values of stiffness, without changing the geometry of the metal cushion pads, several values of the thread wire diameter and degree of compaction (which directly affects the sample density) were used. Thus, three different tread diameters (0.3, 0.4 and 0.5 mm) and two different compaction degrees have been employed (these samples will be referred to as P1-P6). Next, in order to facilitate the reading of the text, Table 1 summarizes the experimental scope of the study ('yes' and 'no' refer the type of experiment each solution was subjected to).

Table 1. Summary of experimental procedures.

Material	**STATIC & DYNAMIC STIFFNESS (*before fatigue phase 1)***	**FATIGUE *Phase 1: $3.5 \cdot 10^5$ cycles***	**STATIC & DYNAMIC STIFFNESS (*after fatigue phase 1 before fatigue phase 2)***	**FATIGUE *Phase 2: $3 \cdot 10^6$ cycles***	**STATIC & DYNAMIC STIFFNESS (*after fatigue phase 2)***	**ELECTRICAL RESISTANCE**	**CORROSION RESISTANCE**
METAL	Yes	Yes	Yes	Yes	Yes	Yes	Yes
METAL P1	Yes	No	No	No	No	No	No
METAL P2	Yes	No	No	No	No	No	No
METAL P3	Yes	No	No	No	No	No	No
METAL P4	Yes	No	No	No	No	No	No
METAL P5	Yes	No	No	No	No	No	No
METAL P6	Yes	No	No	No	No	No	No
EPDM	Yes	Yes	Yes	Yes	Yes	No	No
EVA	Yes	Yes	Yes	Yes	Yes	No	No
TPE-M	Yes	Yes	Yes	Yes	Yes	No	No
TPE-S	Yes	Yes	Yes	Yes	Yes	No	No
TPU	Yes	Yes	Yes	Yes	Yes	No	No
NFU	Yes	Yes	Yes	Yes	Yes	No	No

2.2.- Static and dynamic stiffness.

Static and dynamic stiffness was measured following the guidelines of UNE-EN 13416-9 [32] and UNE-EN 13481-2 [33] standards. In order to properly compare the results of the tests carried out on conventional rail pads and on metallic rubber samples, it was necessary to equalize the dimensions of the specimens. It is beyond current technological capabilities to manufacture metal cushion plates with the dimensions of a standard rail pad. The dimensions of today's rail pads have a very high surface-to-thickness ratio that is

impossible to achieve in metal cushion pads guaranteeing the homogeneity of the material. For this reason, it was decided to modify the dimensions of the rail pads. The surface of a conventional rail pad is 23200 mm^2; in this case, plates of reduced dimensions with a surface of 1811 mm^2 have been used. Consequently, the forces to be applied during the tests according to the standards were reduced proportionally.

Figure 3 summarizes the main features of the static and dynamic stiffness tests and allows the meaning of the parameters that define both tests to be determined. The static stiffness test, see Figure 3 (upper graph), consists in applying three compressive load - unload cycles at a test rate V_e (kN/min), from a minimum load, F_{SP1}, to a maximum value, F_{SPmax}. The static stiffness, k_e, is determined as the loading slope within the third cycle between the loads F_{SP1} and $F_{SP2} = 0.8 \cdot F_{SPmax}$, see formula (1), where d_{sp} is the relative deflection between F_{SP1} and F_{SP2}. To measure the dynamic stiffness, k_d, it is firstly necessary to apply 1000 sine-shaped load cycles between F_{LFP1} and $F_{LFP2} = 0.8 \cdot F_{LFPmax}$, see Figure 3 (lower graph). The tests were carried out at frequencies of 5, 10 and 20 Hz, respectively (which are considered to belong to the low frequency regime). k_d was obtained using the average value of stiffness from the last ten cycles, by means of equation (3). Figure 4 displays the characteristic hysteresis loops which represents both the static and dynamic test performance of the samples during testing. Table 2 summarizes the relevant parameters that define the tests to determine the stiffness.

$$k_e = \frac{F_{SP2} - F_{SP1}}{d_{SP}} \qquad (1)$$

$$k_{d(5/10/20\ Hz)} = \frac{F_{LFP2} - F_{LFP1}}{d_{LFP}} \qquad (2)$$

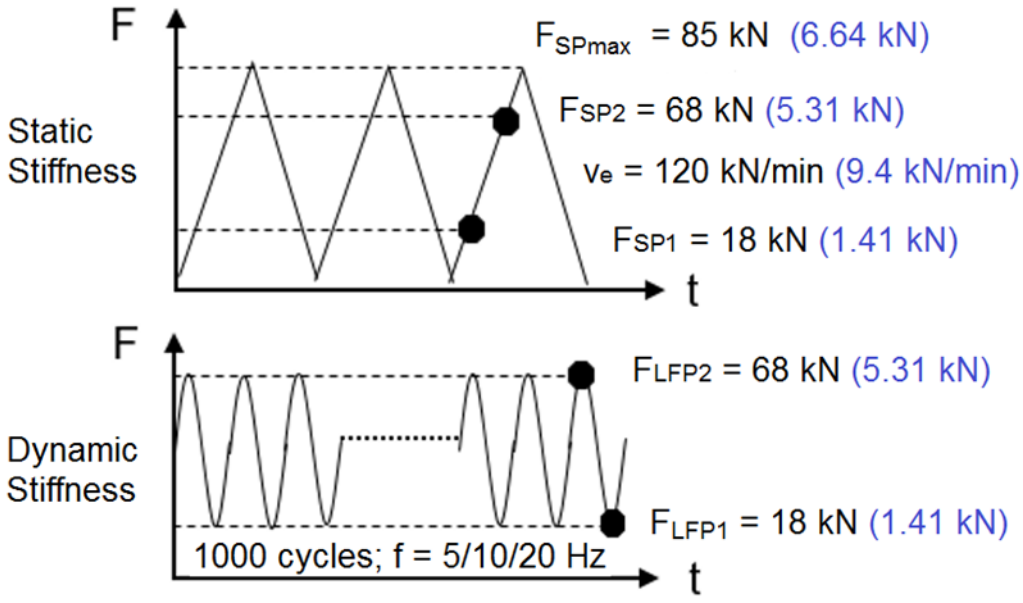

Figure 3. The upper graph describes the static stiffness test, while the features corresponding to the dynamic test are displayed in the lower graph.

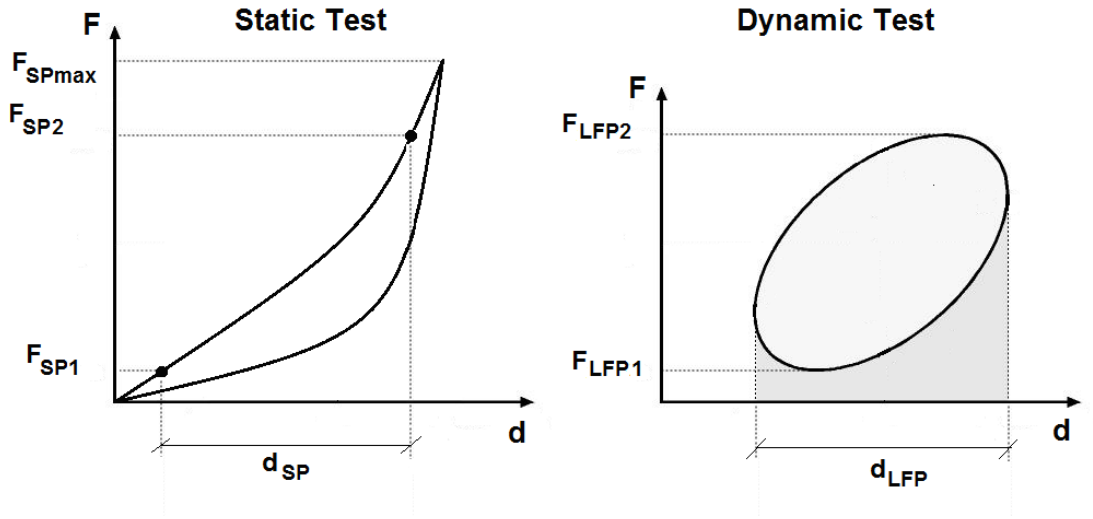

Figure 4. Characteristic hysteresis loops that represents both static and dynamic test performance of the samples.

Table 2. Summary of static and dynamic stiffness test parameters.

	Complete rail pad	**Experimental sample scale**
Surface (mm^2)	23200	1811
F_{SP1}, F_{LP1} (kN)	18	1.41
F_{SP2}, F_{LFP2} (kN)	68	5.31
V_e (kN/min)	120±10	9.4±0.8

Figure 5 shows the experimental setup employed for the tests. The tests were carried out by means of a universal Instron 8800 servo-hydraulic machine, with a loading capacity of ±100 kN under control of loading conditions. Deflection was continuously recorded by means of an LVDT gauge located through the central hole of the sample (see Figure 5).

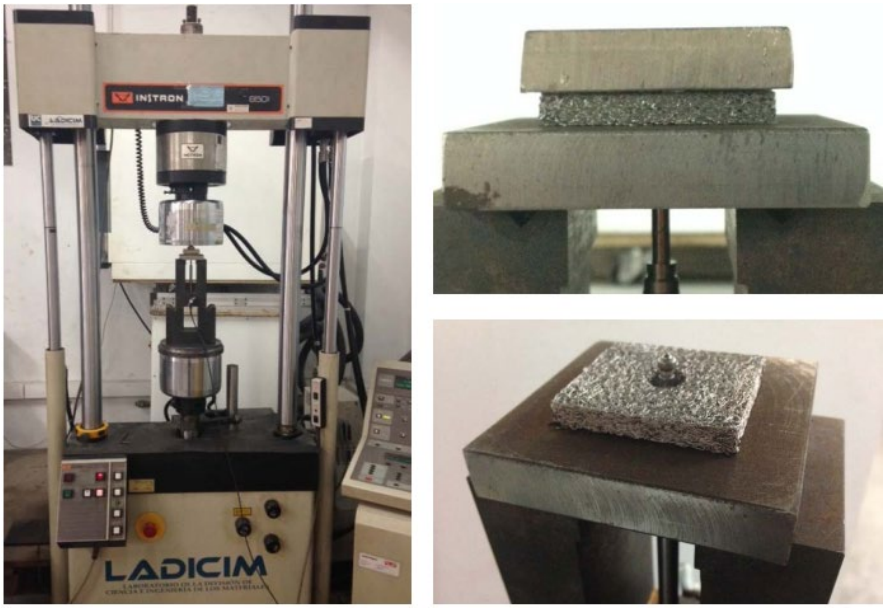

Figure 5. Testing machine and experimental setup designed to perform the tests.

2.3.- Fatigue aging.

The purpose of the fatigue-aging test is to measure the influence of fatigue loading on the material stiffness. The test consists of two stages; firstly, $3.5 \cdot 10^5$ sine-shaped load cycles are applied at a frequency of 5 Hz between the loads F_{LFP1} and F_{LFP2}. Then, the static and dynamic stiffness were determined. The tests were carried out employing the experimental setup shown in Figure 5. The load values applied in the fatigue test are 35% higher than the vertical component of the force used in the standardized fatigue test on inclined sleepers [32]. In addition, in order to verify the performance of the metal cushion pads after long-term fatigue loading, they were subjected to $3 \cdot 10^6$ cycles (with a frequency of 10 Hz, since there is no heating effect induced by the test frequency for metals) with the same loads and then, the static and dynamic stiffness were measured again. As mentioned before, the stiffening process suffered by the polymeric materials over time, after being subjected to fatigue loading, is considered one of the major causes of degradation.

2.4.- Electrical resistance.

One of the advantages behind the use of polymeric materials in rail fastening systems is their intrinsic ability to ensure electrical insulation between rails. For this reason, the electrical resistance of fastening systems with metal cushion pads was measured following the standard UNE-EN 13146-5: 2003 [33]. As sketched in Figure 6, two rail coupons were mounted on a sleeper and electrically connected though a copper wire. The test consists in applying an alternating current (I) and measuring the voltage drop (V) to obtain the electrical resistance (R=V/I).

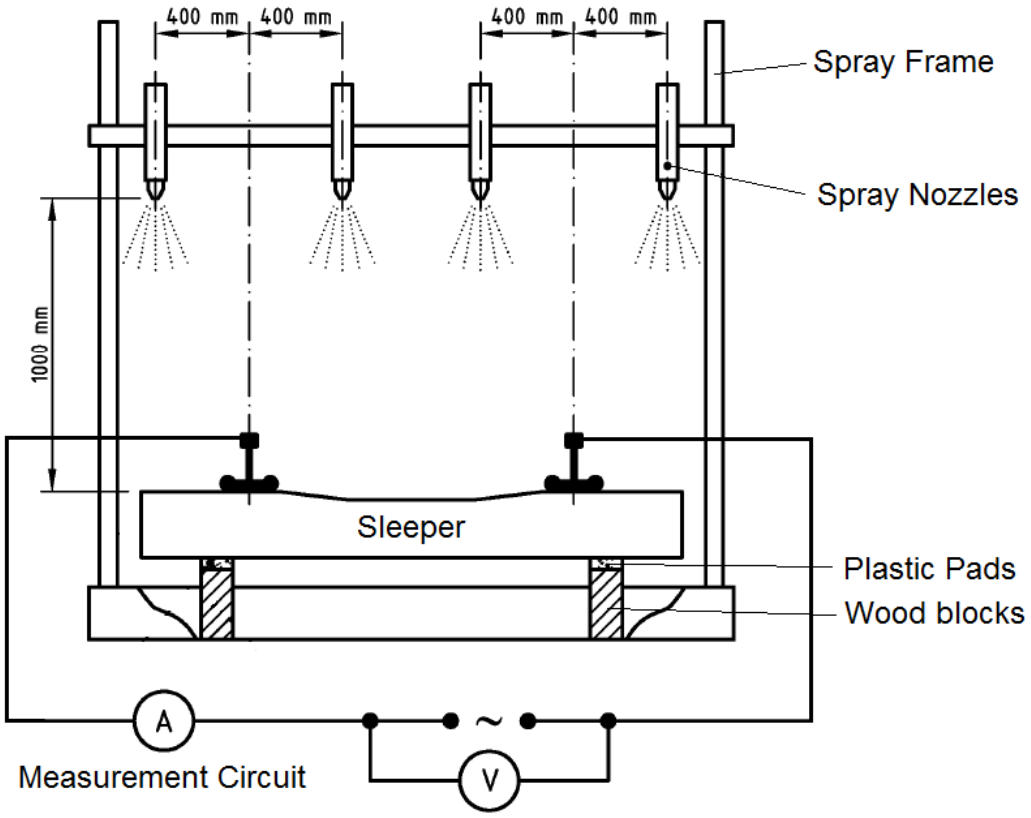

Figure 6. Experimental arrangement employed for the electrical resistance tests.

It is worth noting that these experimental conditions are extremely demanding since the entire assembly is sprayed with water for two minutes and R is continuously recorded for five minutes (two minutes under spraying conditions and three minutes after). This procedure is repeated in 24-hour intervals, a total of three times. The relevant parameters of the test are summarized next:

- Sprayed water conductivity (γ): 20-80 mS / m.
- Water temperature: 15-20°C; environment temperature: 20-25°C.
- Water flow per spray nozzle (q): 8 l / min.
- Spray cone: from 100° to 125° and a nozzle diameter of 3.6 mm.
- Alternating current (AC): 30 V RMS and 50 Hz.

The average of the minimum values of electrical resistance for the three measures, R_γ, is obtained; then, the corrected electric resistance, R_C, is calculated applying $R_C=k_\gamma \cdot R_\gamma$, where k_γ is the correction factor due to the water conductivity ($k_\gamma=0.03 \cdot \gamma$). According to the standard [31], the minimum admissible value for R_C is 5 kΩ.

As shown in Figure 7, nine metal cushion pads were placed between the rail and the sleeper. In addition to this configuration, an alternative solution was characterized, consisting in combining the metal cushion pad with a 1.5 mm thick polyamide plate. This hybrid solution allows the mechanical properties of the metallic

solution to be combined with the insulating ability of the polymer, optimizing in this way the behavior of the component in the short and long term.

Figure 7. Layout of metal cushion samples behind the rail, to perform the electrical resistance test.

2.5.- Corrosion resistance.

Fast-corrosion tests were carried out using the salt spray corrosion test chamber. This kind of tests is currently applied to rail fastener systems according to the standard UNE-EN 13416-5 [37], and following the UNE-EN ISO 9227[34] guidelines. A WEISS TECHNIK SSC - 1000 chamber was employed for the tests, using the following parameters:

- Deionized water with a conductivity of 0.5 µS / cm.
- Sodium chloride of pharmaceutical grade (99% purity).
- Concentration of the solution: 5% by weight of NaCl.
- Test temperature: 35°C.
- Flow rate collected throughout the test: 1.42 ml / hour.
- pH of the solution collected at the end of the test: 7.1.
- Duration of the test: 250 hours.

4. RESULTS AND ANALYSIS

4.1. Static and dynamic stiffness.

The last of the three loading cycles employed to determine the static stiffness is represented in Figure 8(a), making it possible to compare the relative stiffness of the different materials. The first remarkable fact consists of the great difference in stiffness presented by the different materials. As can be seen, the response of the metal cushion solution is between the EVA and the TPE-M solutions. This same pattern of behavior is reproduced in the panel in Figure 8(b, c, d), where the dynamic stiffness of the different materials is represented; in this case three graphs are included, corresponding to the loading frequencies of 5, 10 and 20 Hz. The numerical values are collected in Table 3. It should be noted that static and dynamic behaviors

follow the same trend. Note that, except for a few cases, the order of the materials based on their static and dynamic stiffness is not altered. Thus, the most flexible static solution is EPDM, closely followed by NFU, while the most rigid is EVA (20 times more rigid than the EPDM solution), followed by the metal cushion plate.

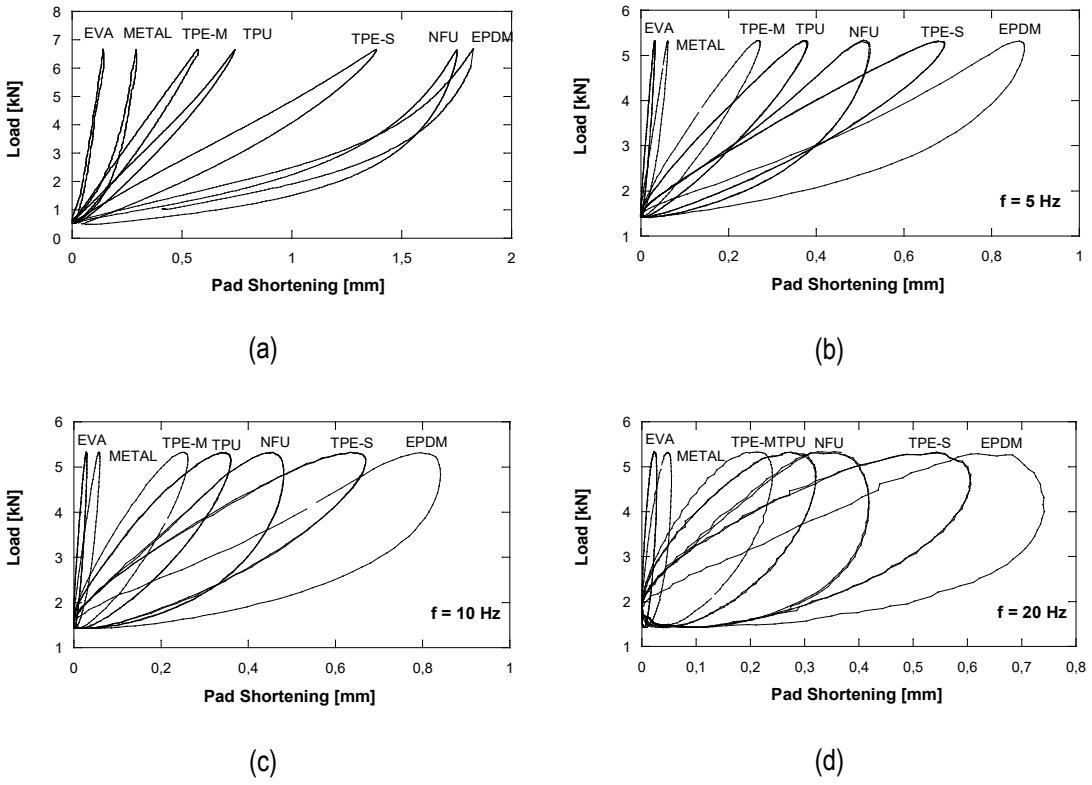

Figure 1. Comparison of the static (a) and dynamic (b, c, d) for frequencies of 5, 10 and 15 Hz, respectively) stiffness of the different solutions characterized.

In order to convey an idea of the differences in response in the static and dynamic regimes, Figure 9 shows the last loading cycles for the static and for the dynamic tests (at different frequencies). This information is expressed numerically in Table 3 where the ratio between the dynamic (average for the three frequencies) and the static stiffness, k_{da}/k_e, is included. This ratio is systematically higher than 1.0, ranging between 1.33 for the TPE-M and 2.64 for the metal cushion pads.

Table 3. Summary of results obtained from the static and dynamic characterization of stiffness.

PAD	k_e [kN/mm]	$k_{d\ 5Hz}$ [kN/mm]	$k_{d\ 10Hz}$ [kN/mm]	$k_{d\ 20Hz}$ [kN/mm]	k_{da} (average k_d) [kN/mm]	k_{da}/k_e
METAL	324.7	806.4	838.9	925.9	857.1	2.64
EPDM	40.8	57.1	59.4	67.4	61.3	1.50
EVA	819.7	1533.7	1655.6	1824.8	1671.4	2.04
TPE-M	146.6	183.8	191.6	208.3	194.6	1.33
TPE-S	54.5	72.1	74.6	82.6	76.4	1.40
TPU	101.4	131.6	138.9	156.3	142.3	1.40
NFU	48.2	95.6	103.7	119.6	106.3	2.20

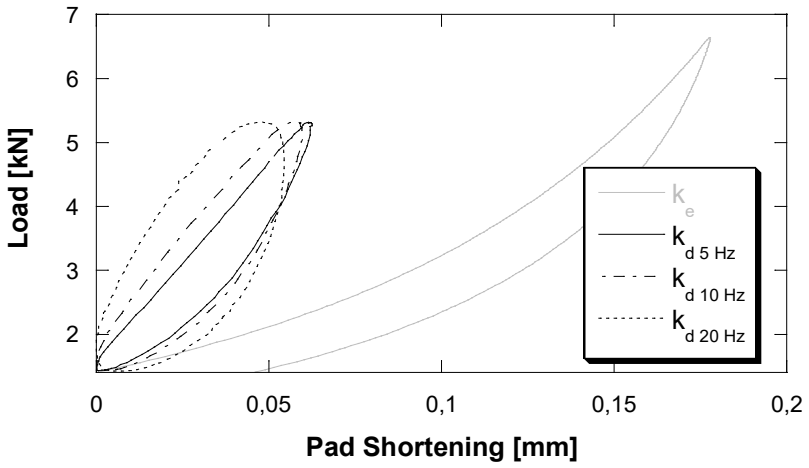

Figure 9. Static and dynamic metal cushion performance.

4.2. Fatigue aging.

The static and dynamic stiffness of new samples were determined after applying $3.5 \cdot 10^5$ sine-shaped load cycles at a frequency of 5 Hz. Table 4 summarizes the results obtained with the same format as Table 3. The relative stiffness variation, represented in Figure 10, is a measure of the degree of alteration undergone by the material because of the cyclical loads applied, as well as an indicator of the stability of its performance under in-service conditions. Note that three groups of responses can be distinguished; on the one hand, TPE-S, TPE-M and EVA have hardly modified their behavior after being subjected to fatigue; on the other

hand, both the static and the dynamic stiffness of EPDM, TPU and NFU have noticeably increased. Finally, the static stiffness of the metal cushion pad ("METAL") has increased while the dynamic performance has hardly been affected. Note that the change in static response of metal cushion are comparable to that of the NFU and less than that of the EPDM.

Table 4. Summary of results obtained from the static and dynamic characterization of stiffness after applying $3.5 \cdot 10^5$ fatigue cycles.

PLATE	k'_e [kN/mm]	$k'_{d\ 5Hz}$ [kN/mm]	$k'_{d\ 10Hz}$ [kN/mm]	$k'_{d\ 20Hz}$ [kN/mm]	k'_{da} (average k_d) [kN/mm]	k'_{da}/k'_e
METAL	362.3	811.7	831.9	896.1	846.6	2.34
EPDM	46.9	65.6	66.7	75.1	69.1	1.47
EVA	833.3	1529	1602.6	1851.1	1660.9	1.99
TPE-M	145.8	181.2	187.3	204.9	191.1	1.31
TPE-S	54.5	71.9	73.2	80.6	75.2	1.38
TPU	107.1	135.1	142	159.2	145.4	1.36
NFU	53.4	112.9	118.5	137	122.8	2.30

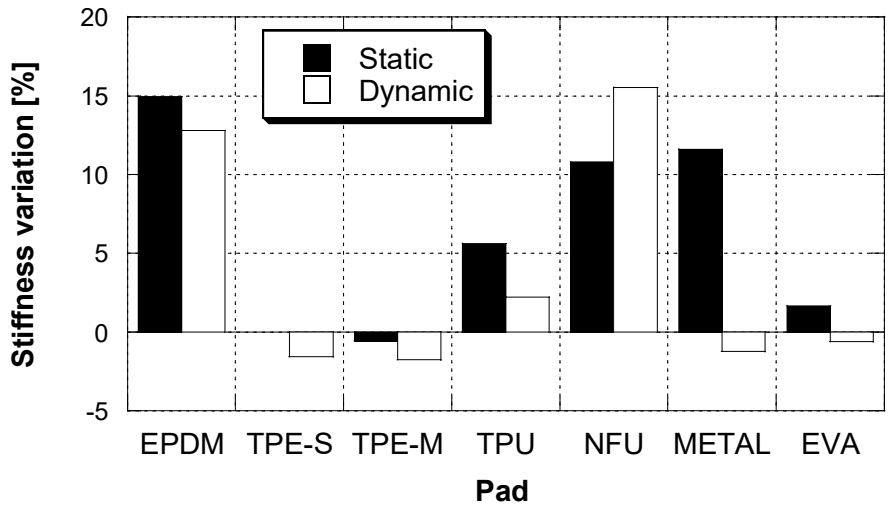

Figure 10. Static and dynamic mechanical properties variation after $3.5 \cdot 10^5$ cycle-fatigue test stiffness results for all samples tested.

Figure 11(a) shows the evolution of the variation in dynamic stiffness throughout the $3.5 \cdot 10^5$ fatigue cycles for the different materials. As can be seen in Figure 11(b), the more flexible the sample is, the more pronounced this variation is. The metallic solution belongs to the group of materials that undergo a reduced variation of stiffness with fatigue. In addition, as the figure suggests, this phenomenon is attenuated, for metallic rubber, for a number of cycles clearly lower than 10^5. On the contrary, in other materials currently used as damping elements in railway lines, such as the NFU, EPDM, TPE-S or TPU, the damage process does not reach a plateau at the end of the test, after applying $3.5 \cdot 10^5$ cycles.

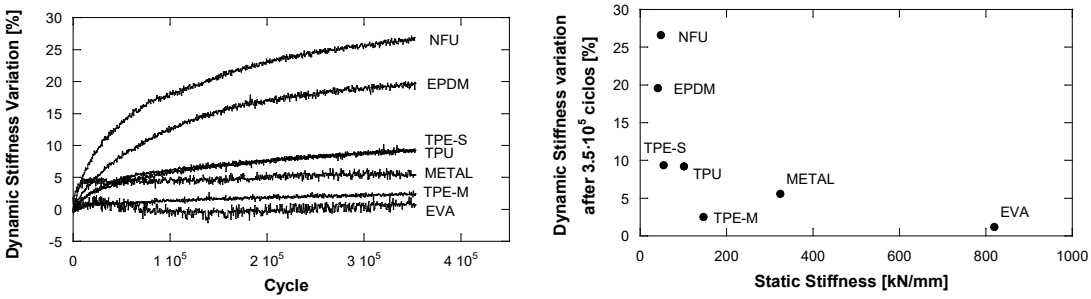

(a) (b)

Figure 11. Dynamic Stiffness variation during $3.5 \cdot 10^5$ cycle-fatigue test.

Ensuring the stability of the behavior of the material against fatigue cycles is an essential requirement for an element that must resist and absorb the loads coming from rail traffic. For this reason, a qualification test of the metallic rubber solution has been carried out under far more demanding conditions. Thus, one of these plates has been subjected to a fatigue test up to $3.0 \cdot 10^6$ cycles, under the same loading conditions as in the previous case, applying a load level 35% higher than that established in the reference standard. The only difference consisted in increasing the frequency to 10 Hz to reduce the duration of the test. Figure 12 shows the evolution of the dynamic stiffness (left) throughout the fatigue test, as well as its relative variation (right). As can be seen, practically all the changes take place for less than $3 \cdot 10^5$ cycles; from that moment on, the properties of the material do not change with the applied loads.

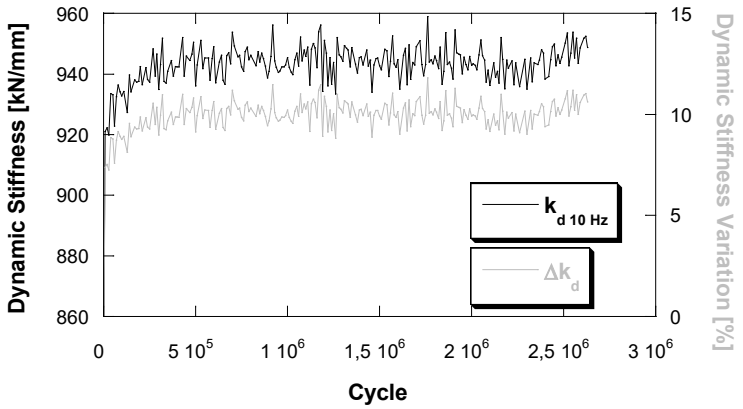

Figure 12. Evolution of the dynamic stiffness (left) and its relative variation (right) of a metal cushion sample as a function of the number of fatigue loads applied.

The stiffness displayed by metal cushion pads, shown in the first part of this study, are relatively high in comparison with current commercial elastomers employed to manufacture standard rail pads. Hence, a strategy to achieve a lower stiffness was developed. The easiest way would consist in increasing the metal cushion pad thickness; nevertheless, this dimension should not exceed a limit of 5 - 6 mm, in order to guarantee the limiting geometric dimensions of the assembly. For this reason, other design parameters were modified aimed at achieving the desired reduction in stiffness. After analyzing with the manufacturer the metal cushion fabrication procedure together, the thread diameter of the stainless wire and the cushion density (amount of wire used) were selected. In this sense, three different diameters (0.3, 0.4 and 0.5 mm, respectively) and two degrees of compaction (porosity) were employed to analyze the influence of these variables on the stiffness. It is worth noting that these prototypes have been manufactured expressly for this study, while the metal pads previously used are commercial parts. The description of these new metal cushion samples and the results obtained in the static and dynamic stiffness tests are collected in Table 5.

Table 5. Description (wire diameter and weight) of the redesigned metal cushion samples as well as the results obtained in the static and dynamic stiffness tests.

Code	Wire Diameter [mm]	Weight [g]	Static Stiffness [kN/mm]	Dynamic Stiffness (5 Hz) [kN/mm]	Dynamic Stiffness (10 Hz) [kN/mm]	Dynamic Stiffness (20 Hz) [kN/mm]	Average Dynamic Stiffness [kN/mm]	k_{da}/k_e
P1	0.5	34.8	501.3	857.7	903.8	1020	927.3	1.85
P2	0.5	45.0	525.6	889.7	960.2	1064	971.3	1.85
P3	0.4	34.3	556.4	894.8	1005	1086	995.3	1.79
P4	0.4	39.2	578.2	1029	1082	1137	1083	1.87
P5	0.3	30.0	776.9	1156	1204	1282	1214	1.56
P6	0.3	35.2	855.1	1388	1427	1567	1461	1.71

The results gathered in the table make it possible to appreciate the influence of the diameter and the weight on the results of static stiffness. Thus, comparing P1, P3 and P6 it is observed that a decrease in diameter leads to an increase in stiffness. On the other hand, the increase in the weight with constant diameter (P1-P2, P3-P4 or P5-P6), also implies an increase in stiffness. In fact, this increase is due to the decrease in the porosity of the element: the spongier the metal cushion is, the lower its rigidity, and vice versa. In addition, the k_d/k_e ratio is reduced in all cases up to a maximum level of 1.87. Figure 13 shows the last cycle of the static stiffness test for the six prototypes tested and Figure 14 a comparison of static and dynamic stiffness for the six samples described in Table 5.

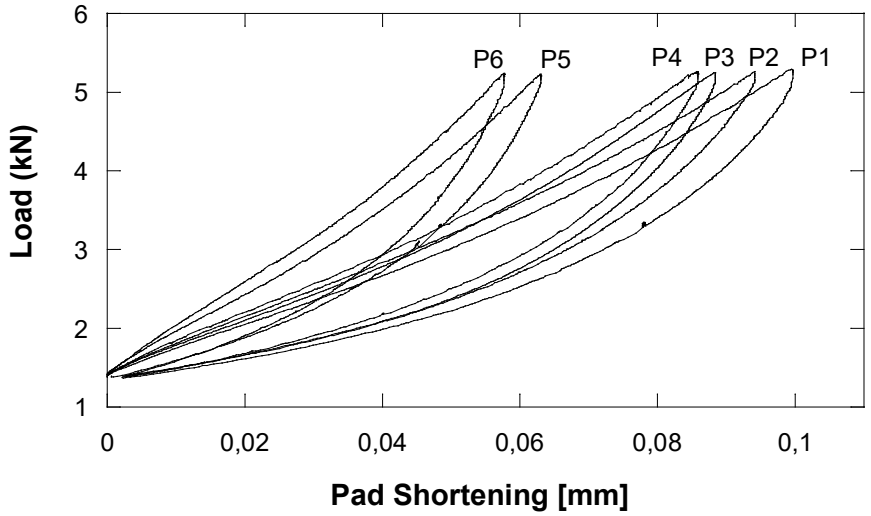

Figure 13. Variation in static stiffness for all samples summarized in Table 5.

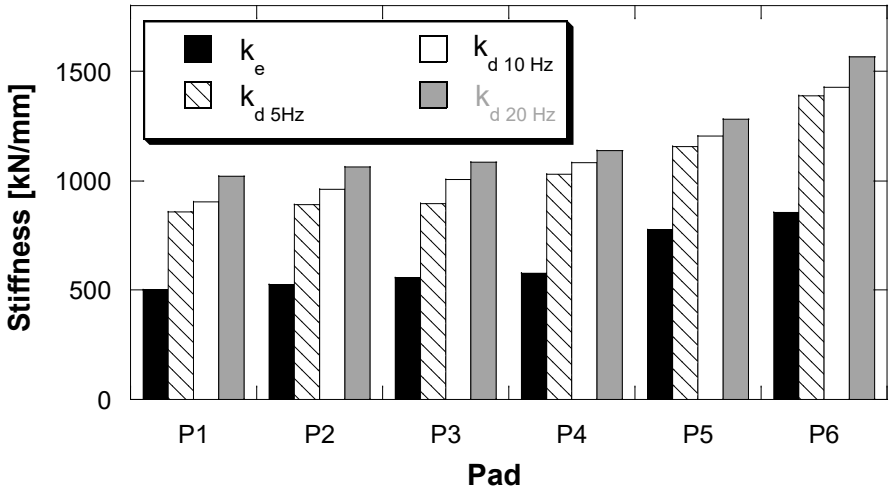

Figure 14. Static and dynamic stiffness for the six prototypes with different wire diameters and weights.

4.3. Electrical resistance.

The electrical conductivity of the water employed in the test was measured, obtaining a value of 36.5 mS/m. The λ factor corresponding to this conductivity is 1.095. Figure 15 shows the time evolution of the electrical current and resistance for three metal cushion samples tested. As can be seen, the resistance decreases below the minimum allowed by the UNE-EN 13146-5 [33] standard (5 kΩ). Moreover, the resistance does not recover after the spraying of the assembly is finished.

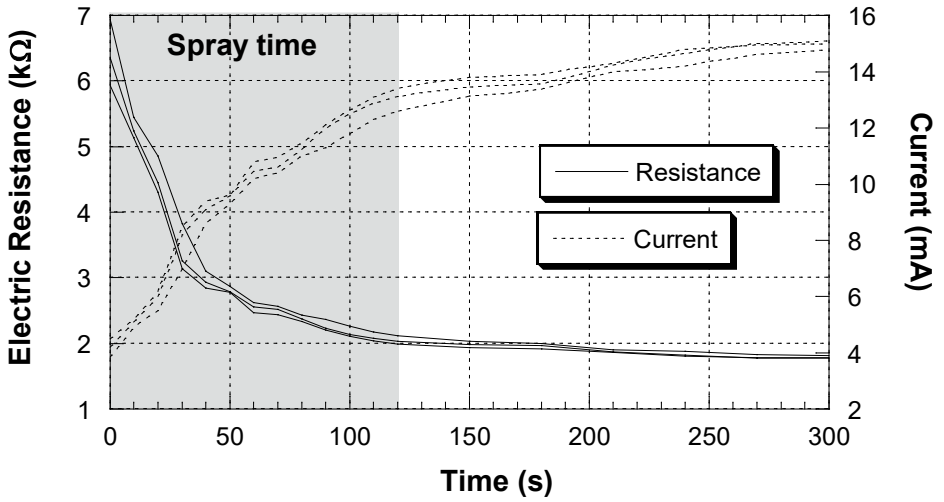

Figure 15. Evolution of electric resistance over time for the free metal cushion pads.

Figure 16 shows the results obtained with three new samples in which a 1.5 mm thick Polyamide 6 plate was placed between the metal cushions and the rail base. A logarithmic scale is employed to display resistance evolution across test time. The results obtained with the isolated metal cushion pad are included in the figure. As can be appreciated, this composite solution fulfills the 5 kΩ limit established by UNE-EN 13146-5 and, moreover, the resistance slightly recovers after the spraying is finished. Table 6 summarizes the results obtained in the electrical tests.

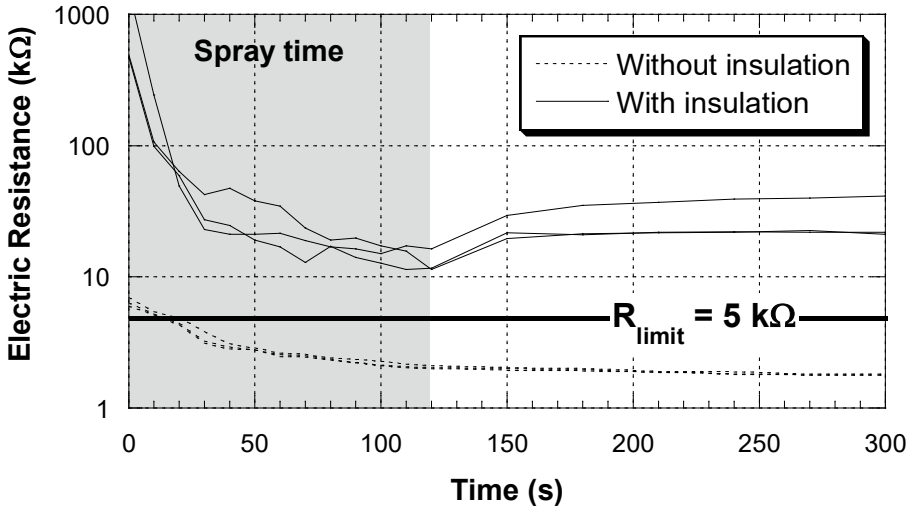

Figure 16. Electric resistance time evolution for the metal cushion fastening with (and without) thin polyamide isolating layer.

Table 1. Summary of resistance values obtained during the two different electric test.

Test	Without insulating PA6 Pad			With insulating PA6 Pad		
	#1	#2	#3	#1	#2	#3
R_{min} (kΩ)	2.11	2.03	1.99	16.4	11.6	11,4
R_C^i (kΩ)	2.31	2.22	2.18	17.9	12.7	12,5
R_C (kΩ)	**2.24** (< 5 kΩ)			**14.4** (> 5 kΩ)		

4.4. Corrosion resistance.

After remaining for 250 hours under the salt spray conditions that define the test, no red corrosion was observed in any of the four samples test. The picture in Figure 17 shows one of the metal cushion pads after the test (the sample was washed in water to remove the residuals of salt accumulated on the surface).

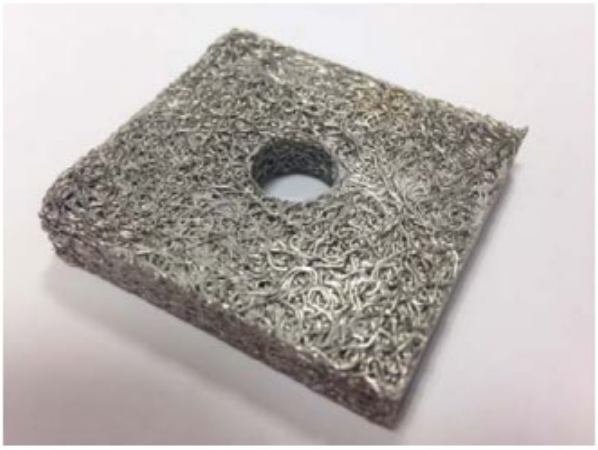

Figure 17. Appearance of a metal cushion sample after 250 hours in salt spray test chamber.

5. CONCLUSIONS

The following list of conclusions summarizes the achievements of the present study regarding the characterization and validation of the metal cushion solution as a viable alternative to replace the current pads based on polymeric materials:

- The results of the static stiffness test have revealed that the metallic cushion solution is slightly stiffer than what is recommended in the literature [4]. However, the tests also show that its static stiffness is between the values of two of the polymer-based solutions, EVA and TPE-M, currently employed. Analogous conclusions are reached from the analysis of the dynamic stiffness tests.
- The results of dynamic hardening (represented as the k_{da}/k_e ratio), suggest the need to increase the flexibility of the metallic solution. In effect, this relationship reaches for the metal cushion pad the

maximum value (k_{da}/k_e = 2.64) among all the alternatives analyzed. Accordingly, a metal cushion constitution with a noticeably lower static stiffness should be obtained in order to avoid reaching too high dynamic stiffness values caused by frequency hardening.

- In spite of the relatively high static stiffness shown by metal cushion pads, they underwent little modifications of stiffness after being subjected to $3.5.10^5$ cycles of fatigue. In addition, it was observed that the most flexible pads, EPDM and NFU, suffer the highest over-stiffening after fatigue while the opposite happens for the least flexible, TPE and EVA, TPU being an intermediate situation. In summary, metal cushion offers a good balance between railway maintenance goals (reasonable flexibility, higher durability)
- The record of dynamic stiffness evolution during the fatigue showed that the metal cushion pads show a slight increase in stiffness in the early cycles of the test, reaching a later stabilization.
- In order to improve the flexibility of the metallic rubber, a series of six samples have been manufactured modifying the diameter of the wire and the density of the mesh. It has been found that both the reduction in diameter and the increase in density lead to an increase in the rigidity of the plate, and vice versa. These results will allow plates to be designed on demand with an appropriate stiffness for the demands under in service conditions.
- The electrical resistance of the metal cushion plates is below the requirements established by the reference standard. However, with the placement of a 1.5 mm polyamide plate, the overall resistance results obtained are comparable to those obtained with a polymer plate.
- The combination of the metal cushion plate with a thin polymeric sheet (~1.5 mm thick) allows the requirement of electrical conductivity to be overcome with ease. This thin sheet would have no structural responsibilities, so that its possible stiffening with time would not affect the overall behavior of the whole. In addition, it would not be directly exposed to the environment, thus avoiding the phenomena of deterioration that affects conventional polymer pad solutions.
- The stainless constitutive material of the metal cushion pad has proved to be highly resistant to environmental corrosion. All the AISI 304 metal cushion samples were able to withstand the 250-hours salt spray test procedure without any sign of rust or damage.

The experimental results obtained confirm that the solution proposed here, based on the metal cushion pad, improves the intrinsic limitations of polymer plates, which in the long term may undergo deterioration associated with environmental conditions (temperature and UV rays) and stiffening by fatigue loading. The hybrid solution based on the combination of a metal cushion pad with a plastic sheet allows the poor electrical insulation ability of the pure metal cushion to be improved, fulfilling the standard requirements. **In this study, other important characteristics, such as the ability to attenuate impacts and vibrations, the characterization of the damping coefficient or the economic viability of this hybrid metal-plastic solution, have not been analyzed. However, in view of the favorable results obtained in this work, these subjects will be the aim of future research. On the other hand, it is worth noting that in this research a purely conceptual solution has been proposed, for the problem of the degradation of the polymers that constitute the seat plates. The proper dimensioning of these novel plates requires additional research, for example to determine the mechanical behavior of the hybrid solution, as well as its long-term response under in-service conditions.**

Although the scope of this study is limited to validating a metal cushion pad prototype, it is important to take into consideration that similar components have been successfully employed in suspension damper systems for passenger seats in railway vehicles. This fact proves the versatility of this solution for different uses, in this specific case, for support elements that must control the rigidity of the superstructure against the high dynamic loads produced by the rail traffic.

As a final remark, it is worth emphasizing that the problems of durability showed by the classical polymer solutions, that motivated this research, will only increase over time. This is particularly concern provided the increasing development that high-speed rail is experiencing worldwide.

6. BIBLIOGRAPHY

[1] M. Sol-Sánchez, F. Moreno-Navarro, and M. C. Rubio-Gómez, "The use of elastic elements in railway tracks: A state of the art review," *Materials (Basel).*, vol. 7, no. 8, pp. 5903–5919, 2014.

[2] E. Kim, S. C. Yang, and S. Y. Jang, "Investigation and Prediction of Stiffness Increase of Resilient Rail Pad due to Train and Environmental Load in High-Speed Railway," in *2015 Joint Rail Conference*, 2015, p. V001T01A035.

[3] D. Álvarez and P. Luque, *Ferrocarriles: ingeniería e infraestructura de los transportes*. Oviedo, 2003.

[4] A. Lopez Pita, "La rigidez vertical de la vía y el deterioro de las líneas de alta velocidad," *Rev. Obras Publicas*, vol. 148, no. 3415, pp. 7–26, 2001.

[5] T. Dahlberg, "Railway track stiffness variations - consequences and countermeasures," *Int. J. Civ. Eng.*, vol. 8, no. 1, pp. 1–12, 2010.

[6] P. F. Teixeira, F. Robuste, and A. Lo, "High speed and track deterioration : the role of vertical stiffness of the track," *Proc. Inst. Mech. Eng. Part F J. Rail Rapid Transit*, vol. 218, no. 1, pp. 31–40, 2004.

[7] R. B, "Dynamic response of elastic fastenings," *Rail Int.*, vol. 17, no. 6, pp. 29–36, 1986.

[8] W. S. Günther Leykauf, "Untersuchungen Und Erfahrungen Mit Besohlten Schwellen," *EI - Der Eisenbahningenieur*, 2004.

[9] K. Giannakos, "Influence of Rail Pad Stiffness on Track Stressing, Life-Cycle and Noise Emission," *Second Int. Conf. Sustain. Constr. Mater. Technol. June 28 - June 30, 2010, Univ. Politec. delle Marche, Ancona, Italy. Spec. Proc.*, no. Figure 2, 2010.

[10] S. Kaewunruen and A. M. Remennikov, "Sensitivity analysis of free vibration characteristics of an in situ railway concrete sleeper to variations of rail pad parameters," *J. Sound Vib.*, vol. 298, no. 1–2, pp. 453–461, Nov. 2006.

[11] S. Kaewunruen and A. M. Remennikov, "Response and prediciton of dynamic characteristics of worn rail pads under static preloads," *Proc. 14th Int. Congr. Sound Vib.*, no. July, pp. 9–12, 2007.

[12] J. Maes, H. Sol, and P. Guillaume, "Measurements of the dynamic railpad properties," *J. Sound Vib.*, vol. 293, no. 3–5, pp. 557–565, 2006.

[13] T. X. Wu, "On the railway track dynamics with rail vibration absorber for noise reduction," *J. Sound Vib.*, vol. 309, no. 3–5, pp. 739–755, 2008.

[14] D. Thompson, *Railway Noise and Vibration*, 1st Editio. 2008.

[15] N. Vincent, P. Bouvet, D. J. Thompson, and P. E. Gautier, “Theoretical Optimization of Track Components To Reduce Rolling Noise,” *J. Sound Vib.*, vol. 193, no. 1, pp. 161–171, 1996.

[16] T. X. Wu and D. J. Thompson, “The effects on railway rolling noise of wave reflections in the rail and support stiffening due to the presence of multiple wheels,” *Appl. Acoust.*, vol. 62, no. 11, pp. 1249–1266, 2001.

[17] S. Kaewunruen and A. M. Remennikov, “An Experimental Evaluation of the Attenuation Effect of Rail Pad on Flexural Behaviour of Railway Concrete Sleeper under Severe Impact Loads,” *Australas. Struct. Eng. Conf.*, no. 51, pp. 26–27, 2008.

[18] I. A. Carrascal Vaquero, “Atenuación frente a impacto en sistemas de sujeción ferroviaria de alta velocidad.”

[19] G. X. Chen, W. J. Qian, J. L. Mo, and M. H. Zhu, “Influence of the rail pad stiffness on the occurrence propensity of rail corrugation,” *J. Vib. Eng. Technol.*, vol. 4, no. 5, 2016.

[20] J. I. Egana, J. Vinolas, and M. Seco, “Investigation of the influence of rail pad stiffness on rail corrugation on a transit system,” vol. 261, no. 2, pp. 216–224, Jul. 2006.

[21] I. A. Carrascal Vaquero, “Optimization and analysis of the performance of clamping systems for Spanish high speed railways,” 2006.

[22] P. Lindley, “Natural Rubber in Civil Engineering,” *Rubber World*, vol. 161, no. 4, pp. 56–61, 1970.

[23] T. Sawada and M. Watanabe, “Investigation on the durability of test rail pads by the field and quality tests,” *Q. Rep. RTRI (railw. Tech. Res. Institute)*, vol. 20, no. 1, 1979.

[24] S. Kaewunruen, “Monitoring structural degradation of rail pads in laboratory using impact excitation technique,” no. June 2015, pp. 389–394, 2005.

[25] G.-S. F. Carrascal I, Casado JA, Diego S, Polanco JA, “Efecto del envejecimiento de placas de asiento de carril inyectadas con TPE en la elasticidad de la vía para Alta Velocidad,” 2010.

[26] I. A. Carrascal, J. A. Casado, J. A. Polanco, and F. Gutiérrez-Solana, “Dynamic behaviour of railway fastening setting pads,” *Eng. Fail. Anal.*, vol. 14, no. 2, pp. 364–373, 2007.

[27] I. A. Carrascal, J. A. Casado, J. A. Polanco, and F. Gutiérrez-Solana, “Comportamiento dinámico de placas de asiento de sujeción de vía de ferrocarril,” *Análisis mecánica la Fract.*, vol. 22, pp. 372–377, 2005.

[28] I. A. Carrascal, J. A. Casado, S. Diego, and J. A. Polanco, “Dynamic behaviour of high-speed rail fastenings in the presence of desert sand,” *Constr. Build. Mater.*, vol. 117, pp. 220–228, Aug. 2016.

[29] M. Sol-Sánchez, F. Moreno-Navarro, and M. C. Rubio-Gámez, “The use of deconstructed tire rail pads in railroad tracks: Impact of pad thickness,” vol. 58, pp. 198–203, 2014.

[30] AEN/CTN 25 - APLICACIONES FERROVIARIAS, “UNE-EN 13146-9:2011+A1:2012 - Aplicaciones ferroviarias. Vía. Métodos de ensayo de los sistemas de fijación. Parte 9: Determinación de la rigidez.,” 2012.

[31] AENOR, “UNE-EN 13481-2. Railway applications. Track. Performance requirements for fastening systems. Part 2: Fastenig systems for concrete sleepers.” 2010.

[32] AENOR, “UNE-EN 13146-4. Railway applications. Track. Test methods for fastening systems. Part 4: Effect of repeated loading.” 2015.

[33] AENOR, “UNE-EN 13146-5 Railway applications. Track. Test methods for fastening systems - Part 5: Determination of electrical resistance.” 2012.

[34] AENOR, “UNE-EN ISO 9227. Corrosion tests in artificial atmospheres. Salt spray tests,” 2012.

[35] ADIF, *ET 03.360.570.0 Placas elásticas de asiento para sujeción VM*. 2005.

[36] A. Perez, “www.silentflex.com,” 2015. .

[37] AENOR, “UNE-EN 13146-6. Railway applications. Track. Test methods for fastening systems. Part 6: Effect of severe environmental conditions,” 2012.